2019

Ca2+ Entry via TRPC1 is Essential for Cellular Differentiation and Modulates Secretion via the SNARE Complex

Thad A. Rosenberger
University of North Dakota, thad.rosenberger@UND.edu

Anne Schaar

Yuygang Sun

Pramod Sukumaran

Danielle Krout

See next page for additional authors

Ca^{2+} entry via TRPC1 is essential for cellular differentiation and modulates secretion via the SNARE complex

Anne Schaar[1,2], Yuyang Sun[1,3], Pramod Sukumaran[1,3], Thad A. Rosenberger[1], Danielle Krout[4], James N. Roemmich[4], Lutz Brinbaumer[5], Kate Claycombe-Larson[4*], and Brij B. Singh[1,3*]

[1]Department of Biomedical Science, School of Medicine and Health Sciences, University of North Dakota, Grand Forks, ND 58203, USA.
[2]Present address: University of Wisconsin-Madison, Madison, WI 53705
[3]Present address University of Texas Health San Antonio, San Antonio TX 78229.
[4]US Department of Agriculture-Agricultural Research Service, Grand Forks Human Nutrition Research Center, Grand Forks, ND 58203, USA.
[5]Neurobiology Laboratory, NIHES, NIH, 111 TW Alexander Dr., Research Triangle Park, NC 27709, USA and Institute of Biomedical Research, (BIOMED) Catholic University of Argentina, Av. Alicia Moreau de Justo 1300, Edificio San Jose Piso 3, Buenos Aires C1107AAZ, Argentina.

*Correspondence: brij.singh@med.und.edu (B.B.S), kate.larson@ars.usda.gov (K.C.-L.)

Key words: TRPC1; Ca^{2+} entry; adipocytes differentiation; adiponectin secretion; metabolic homeostasis

JCS Advance Online Article. Posted on 10 June 2019

Abstract

Adipocyte functionality, including adipocyte differentiation and adipokine secretion, is essential in obesity-associated metabolic syndrome. Here, we provide evidence that Ca^{2+} influx in primary adipocytes, especially upon store-depletion, plays an important role in adipocyte differentiation, functionality, and subsequently metabolic regulation. The endogenous Ca^{2+} entry channel in both subcutaneous and visceral adipocytes was dependent on TRPC1-STIM1 and blocking Ca^{2+} entry with SKF-96365 or $TRPC1^{-/-}$ derived adipocytes inhibited adipocyte differentiation. Additionally, $TRPC1^{-/-}$ mice have decreased organ weight, but increased adipose deposition and reduced serum adiponectin and leptin concentrations, without affecting total adipokine expression. Mechanistically, TRPC1-mediated Ca^{2+} entry regulated SNARE complex formation and agonist –mediated secretion of adipokine loaded vesicles was inhibited in $TRPC1^{-/-}$ adipose. These results suggest an unequivocal role of TRPC1 in adipocytes differentiation and adiponectin secretion, and loss of TRPC1 disturbs metabolic homeostasis.

Summary Statement: TRPC1 modulates Ca^{2+} entry that is essential in adipocytes differentiation and adiponectin secretion via facilitating SNARE complex formation and maintains metabolic homeostasis.

Introduction

Adipose tissue (AT) was initially considered an inert fat storage depot until the discovery of linkages between obesity and inflammation (Rosen and Spiegelman, 2006). Currently, AT is considered a complex endocrine organ secreting over 600 bioactive factors (Lehr et al., 2012; MacDougald and Burant, 2007), termed adipokines. Adipokines influence diverse physiological processes by relaying information to other metabolically active organs such as muscle, liver, pancreas and brain, thereby modulating systemic metabolism (Ouchi et al., 2011). Importantly, increased adipose accumulation, as seen in obesity, correlates to dysregulation of adipokine secretion (Arita et al., 1999; Matsuzawa, 2010) and increases susceptibility to other diseases (Rasouli and Kern, 2008). Altering levels of the adipokines, mainly adiponectin (Fruebis et al., 2001; Okada-Iwabu et al., 2013) and leptin (Stern et al., 2016), have shown to improve energy homeostasis and offset diet-induced obesity. Thus, adipokines have potential to be therapeutic targets to combat/counter or reduce obesity and other metabolic diseases; however, a full understanding of the mechanisms and intracellular mediators that modulate adipokine secretion within AT is first required.

Secreted, adiponectin occurs in three isoforms, a low or medium molecular weight trimer-dimer and an oligomeric complex of greater molecular weight, that modulate diverse physiological functions including thermogenesis (Hui et al., 2015) and sensitizing insulin signaling (Yamauchi et al., 2001). Regulated exocytosis in adipocytes mediates key functions, exemplified by insulin-stimulated secretion of peptides such as adiponectin and recycling of intracellular membranes containing GLUT4 glucose transporters to the cell surface (Bogan and Lodish, 1999). Release of adiponectin from adipocytes has been shown to be insulin and Ca^{2+} dependent (Bogan and Lodish, 1999; Cong et al., 2007; Komai et al., 2014; Xie et al., 2008) and a high-Ca^{2+} diet has been shown to stimulate the expression of adipokines along with inhibition of pro-inflammatory factors (Sun and Zemel, 2007),

however the molecular mechanism and relationship with Ca^{2+} channels is not known. Adiponectin is initially synthesized as a pre-hormone, oligomerized into three isoforms and stored in vesicles until stimulated release. Plasma membrane SNAP-25 and syntaxin, termed t-SNAREs, and secretory vesicle-associated protein VAMP or v-SNARE, are part of the conserved protein complex involved in fusion of opposing membranes necessary for exocytosis. It has been demonstrated that Ca^{2+} provides the final event needed for vesicle fusion and release of its content (Brose et al., 1992).

Several studies have shown that anatomical distribution of adipose tissue dictates differing characteristics where subcutaneous adipocytes have distinct metabolic properties from visceral adipocytes (Baglioni et al., 2012). Proliferation of the subcutaneous adipose tissue (Subc AT) may be considered beneficial, in part, by increasing “healthy” lipid storage capacity that produces fewer inflammatory cytokines. Whereas, visceral adipose tissue (VAT) is thought to be more inflammatory (Kadiri et al., 2017; O'Rourke et al., 2009) and leads to the development of obesity and related metabolic diseases (Foster et al., 2011; Seale et al., 2011). Although the debate about the metabolic function of Subc AT and VAT is not yet settled (Fabbrini et al., 2010; Thörne et al., 2002), variances in distribution of lipids in Subc AT and VAT could be critical in the development of metabolic diseases. One such area to investigate regarding variances between Subc AT and VAT tissues could be the process of differentiation of committed preadipocytes into mature adipocytes. Interestingly, it has been shown that differentiation is impaired in Subc preadipocytes of obese subjects and their ability to differentiate is negatively correlated to BMI and cell size (Isakson et al., 2009). Further, in an obese state, the preadipocyte to mature adipocyte ratio is reduced and the ability of Subc AT to differentiate properly may be diminished pushing the accumulation of fat to visceral depots (Tchoukalova et al., 2007). Similar results have shown an age-dependent decline in differentiation and increases in adipose tissue accumulation in obesity is likely due to hypertrophy instead of hyperplasia (Kim et al., 2014). Although several nuclear receptors and transcription factors that

regulate adipocyte differentiation and adipogenesis have been identified (Farmer, 2006), factors upstream to the activation of these transcription factors are still unknown. The activation of peroxisome proliferator–activated receptor γ (PPARγ) occurs in the intermediate or late stage of adipogenesis, and PPARγ activation has been determined to be a master regulator of adipogenesis (Haider et al., 2017). PPARγ has been linked to the transcription of genes expressed in mature adipocytes such as fatty acid binding protein (FABP4), required for transport of free fatty acids, and perilipin (PLIN1), covers the surface of mature lipid droplets in adipocytes and regulates lipolysis. Calcium has been identified as important for the transcriptional regulation of adipocyte differentiation; however, the molecular identity of the Ca^{2+} channel has yet to be identified. Studies on preadipocytes show that elevating $[Ca^{2+}]_i$ early in differentiation inhibits PPARγ induction and triglyceride accumulation (Neal and Clipstone, 2002).

Ca^{2+} is an important secondary messenger molecule involved in regulating numerous cell processes including cell proliferation and differentiation, gene transcription, and exocytosis(Berridge et al., 2000) and is controlled by altering intracellular Ca^{2+} concentrations ($[Ca^{2+}]_i$). Changes in $[Ca^{2+}]_i$ are the result of either the release of Ca^{2+} stored in the endoplasmic reticulum (ER) that initiates store-operated Ca^{2+}entry (SOCE) (Parekh and Putney, 2005; Putney et al., 2017) or direct Ca^{2+} entry from the extracellular space mediated by various types of channels including voltage-gated Cav channels (Catterall, 2000) and channels belonging to the 7-member TRPC family (Birnbaumer et al., 1996). During SOCE mechanisms, ER Ca^{2+} stores are depleted and the ER protein Stromal interaction molecule 1 (STIM1) approaches the plasma membrane where it interacts with ORAI1 (Feske et al., 2006) and Transient Receptor Potential Canonical 1 (TRPC1) channels (Asanov et al., 2015; Liao et al., 2008) resulting in Ca^{2+} influx and increased $[Ca^{2+}]_i$. Microarray analysis has shown both TRPC1 and TRPC5 expression are induced when adipocytes mature; however the physiological characterization of the Ca^{2+} entry channel in subcutaneous and visceral adipocytes is still missing.

The aim of this study was to identify the endogenous Ca^{2+} entry channel in adipocytes cells and establish its physiological function in modulating adipocytes differentiation and adipokine secretion. We report for the first time the AT-dependent differences in sensitivity to SOCE, differentiation, and lipid accumulation. We further report that the endogenous Ca^{2+} entry channel in adipocytes is dependent on TRPC1 and loss of TRPC1 function inhibits adipocyte differentiation. Furthermore, loss of TRPC1 inhibited vesicular fusion by SNARE proteins and $TRPC1^{-/-}$ mice exhibited increased adipose deposition along with having reduced serum adiponectin and leptin concentrations. Together these results suggest TRPC1 is essential for adipocytes differentiation and adipokine secretion, which regulates metabolic homeostasis to reduce obesity.

Results

SOCE is essential for the differentiation of subcutaneous adipocytes

To establish the molecular identity of the SOCE channel in adipose cells, we evaluated Ca^{2+} signaling in isolated stromal vascular fraction (SVF) of mouse adipose tissue (AT). Addition of thapsigargin (1μM, Tg), a SERCA pump blocker that causes loss of Ca^{2+} from the internal ER stores, showed a small increase in intracellular Ca^{2+} ($[Ca^{2+}]_i$) levels (first peak) in subcutaneous adipose tissue (Subc AT) SVF cells (Fig. 1A, B). In the presence of 1mM external Ca^{2+}, Subc AT SVF cells showed a significant increase in $[Ca^{2+}]_i$ levels (second peak), indicating the presence of store-mediated Ca^{2+} entry (Fig. 1A, B). Importantly, Subc AT SVF cells treated with SKF96365 (10μM SKF, a blocker of store-mediated Ca^{2+} influx channels) were observed to have a significant reduction in SOCE without any change in internal ER Ca^{2+} release (Fig. 1A, B). To establish the molecular identity of the Ca^{2+} influx channel in Subc AT

cells, electrophysiological recordings of membrane currents were performed. Addition of Tg induced an inward current, which was non-selective in nature and reversed between 0 and -5 mV (Fig. 1C, D). The current properties observed in Subc AT SVF cells were similar with previous recordings observed with TRPC1 channels (Liu et al., 2004; Selvaraj et al., 2012; Shi et al., 2012; Yuan et al., 2007). Moreover, pretreatment with SKF, 2APB, or BTP2 significantly inhibited the Tg-induced nonselective current (Fig. 1 C-E), suggesting that in Subc AT SVF cells, the SOCE is dependent on TRPC1 channels.

We next evaluated the physiological properties of the SOCE channels in differentiated adipocytes from Subc AT. Samples taken from both Subc AT deposits were cultured and differentiated into mature adipocytes *ex vivo*. Similar to the observed response by Subc AT SVF cells, differentiated Subc adipocytes showed no change in the ER Ca^{2+} release (upon addition of Tg, 1μM) (Fig. 1F,G). Addition of 1mM external Ca^{2+} also showed an increase in $[Ca^{2+}]_i$ levels, which were significantly higher than non-differentiated cells (Fig.1A,B), but was also reduced when treated with SKF as compared to untreated differentiated control (Fig. 1F,G). Furthermore, a similar TRPC1-like current was observed in differentiated Subc AT adipocytes and the Tg-induced currents were again inhibited by SKF (Fig. 1H-J). Comparison of Subc AT SVF to differentiated Subc AT adipocytes indicated a ~25% increase in amplitude of TRPC1-like currents in differentiated Subc AT (Fig. 1E, J). To identify the expression of calcium channels in modulating SOCE, protein expression of TRPC1, STIM1, and ORAI1 in both Subc AT SVF and differentiated Subc AT was analyzed. Consistent with other studies, expression of TRPC1 and STIM1 was increased upon differentiation (Graham et al., 2009; Sukumar et al., 2012); however, there was no change in ORAI1 expression (Fig. 1K,L). Known markers of adipocyte differentiation, FABP4 and Perilipin, were used to confirm differentiation. Interestingly, altering $[Ca^{2+}]_i$ inhibits differentiation of adipocytes (Jensen et al., 2004), thus we speculated whether blocking SOCE using SKF would have a similar effect. Subc AT SVF adipocytes were differentiated in the presence of SKF (10 μM) for 7 days and lipid accumulation was detected by oil-red-o (Fig. 1M, N). Treatment with SKF

significantly reduced the ability of Subc AT SVF cells to accumulate intracellular lipids. In addition, SKF treatment reduced expression of differentiation markers FABP4, Perilipin, and PPARγ further indicating the involvement of Ca^{2+} influx via SOCE channels in adipocyte differentiation (Fig. 1O, P). Interestingly, cell cycle was also affected and SKF treatment significantly increased G2-M phase (Fig. 1Q). Together these results indicate that SOCE in Subc AT is dependent on TRPC1 before and after differentiation and may have an important role in the mechanisms of differentiation and lipid accumulation.

Differentiated visceral adipocytes exhibit increased in SOCE

White AT has different properties based on its location. It is well known that visceral adipose tissue (VAT), when compared with Subc AT, is functionally different in that VAT has higher inflammatory potential (Zhou et al., 2007) due to increased localization of inflammatory and immune cells. VAT has greater oxidative capacity and lipolysis potential than Subc AT and less capacity to differentiate resulting in a greater percentage of large adipocytes as compared to Subc AT (Ibrahim, 2010). To date, it is unknown whether store-mediated changes in $[Ca^{2+}]_i$ leading to adipocyte differentiation is analogous between VAT and Subc AT. Thus, we investigated SOCE from adipocytes derived from the VAT depots. Consistent with Subc AT protein expression, STIM1, ORAI1 and TRPC1 were expressed in both VAT SVF and differentiated VAT adipocytes with increased expression of STIM1 and TRPC1 seen in differentiated VAT with no change in ORAI1 expression (Fig. 2A, B). Membrane current recordings of VAT SVF adipocytes induced upon the addition of Tg (1μM) showed an inward TRPC1-like current and pretreatment with SKF (10μM) significantly inhibited the nonselective current (Fig. 2C-E). Importantly, after differentiation, the similar TRPC1-like current was observed in VAT cells (Fig. 2F-H) and a ~50% increase in the current amplitude was observed upon differentiation (Fig. 2E, H). Again Tg-induced currents were inhibited by the addition of SKF in differentiated VAT adipocytes, however the residual current observed was similar to I_{crac} currents (Fig. 2F-H). The effect of SKF on lipid

accumulation was also evaluated in differentiating VAT SVF adipocytes with the addition of 10 μM SKF (Fig. 2K). Similar to Subc AT, addition of SKF significantly reduced the ability of VAT to accumulate intracellular lipids as well as a reduced protein expression of differentiation markers (Fig. 2I-J). Calcium imaging of VAT SVF adipocytes treated with SKF had no change in internal Ca^{2+} release, but had a significant reduction in SOCE (Fig. 2L-M). However, differentiated VAT adipocytes treated with SKF showed a reduction in both internal Ca^{2+} ER store release upon Tg treatment and SOCE upon addition of external Ca^{2+} (Fig. 2N-O). These results indicate that differentiated VAT adipocytes may be more sensitive to alterations in SOCE than VAT SVF adipocytes, however the properties of the SOCE and role in differentiation and lipid accumulation are similar between Subc AT and VAT.

TRPC1$^{-/-}$ mice have increased adiposity with age

Both the increase in TRPC1 expression upon adipocyte differentiation and the reduction in SOCE observed when TRPC1 is blocked led us to investigate whether dysfunctional TRPC1 channels could alter overall body composition. Utilizing our homozygous TRPC1 knockout mice (TRPC1$^{-/-}$), we confirmed the absence of TRPC1 in Subc AT by assessing TRPC1 mRNA and protein expression, without any change in TRPC3 mRNA (Fig. 3A). Body mass composition analysis was performed on TRPC1$^{-/-}$ and WT mice aged 13-15 months, which resulted in a more than two-fold increase in the ratio of total fat to body weight in TRPC1$^{-/-}$ mice as compared to WT mice (Fig 3B). Visually this difference in body composition can be seen in Figure 3C where TRPC1$^{-/-}$ mice have increased Subc AT and VAT volume as compared to its WT counterpart. Interestingly, the increase in total fat observed in TRPC1$^{-/-}$ mice did not translate to an increase in their overall body weight. Within a majority of age groups, no significant difference in the overall body weight was observed in TRPC1$^{-/-}$ when compared with WT mice, however in TRPC1$^{-/-}$ there seems to be a greater trend of age-related increased body mass (Fig 3D). Further, no difference in food consumption nor lean body mass/skeletal muscle mass was observed (data not shown). TRPC1$^{-/-}$ mice did, however, have lower organ weights (such as hearts and kidneys), which were reduced in size regardless of age and may attribute to the increase in

adiposity without an increase in overall body weight (Fig 3E). Protein expression analysis of numerous Ca^{2+} regulating proteins in Subc AT and VAT was also performed to rule out compensation for the lack of TRPC1. As shown in Figure 3F-I, no change in expression was observed between WT and TRPC1$^{-/-}$ AT indicating the lack of TRPC1 function in AT most likely does not change protein expression of other Ca^{2+} channels. Together these data suggest that the loss of TRPC1 function attributes to an increase in the accumulation of adipocytes, but not overall weight. Furthermore, the loss of TRPC1 function is not compensated by other TRPCs and ORAIs in AT.

Loss of TRPC1 in adipocytes reduces SOCE and ability to differentiate

To confirm that the loss of TRPC1 negatively effects SOCE fluctuations within Subc AT and VAT, SVF cells from TRPC1$^{-/-}$ and WT mice were isolated and differentiated into adipocytes. Analysis by Ca^{2+} imaging of both Subc AT cell types (SVF and differentiated adipocytes) showed TRPC1$^{-/-}$ cells had a reduction in internal ER Ca^{2+} release (first peak) with the addition of Tg as compared to WT (Fig. 4A, B, F, G). When external Ca^{2+} was added, $[Ca^{2+}]_i$ in both SVF and differentiated TRPC1$^{-/-}$ cells was significantly reduced indicating diminished SOCE in TRPC1$^{-/-}$ cells. Consistent with these results, TRPC1 currents were significantly reduced in Subc AT SVF in TRPC1$^{-/-}$ mice (Fig. 4C-E). Similar results were observed in differentiated Subc AT, where loss of TRPC1 significantly decreased Tg-mediated Ca^{2+} currents (Fig. 4H-J). As shown in Figures 1 and 2, modifying $[Ca^{2+}]_i$ affects adipocyte differentiation, thus we investigated whether a lack of TRPC1 would alter the ability of TRPC1$^{-/-}$ Subc SVF cells to differentiate. Analysis of lipid accumulation in WT and TRPC1$^{-/-}$ Subc AT after differentiation revealed a significant reduction in total lipid when TRPC1 is nonfunctional (Fig. 4K, L). Protein expression of Perilipin, FABP4, and PPARγ were also reduced in TRPC1$^{-/-}$ Subc AT as compared to WT with significance found in PPARγ and Perilipin (Fig. 4M,N). To offset the reduced $[Ca^{2+}]_i$ of TRPC1$^{-/-}$ cells, Subc AT SVF cells from WT and TRPC1$^{-/-}$ mice were differentiated with a 2 and 4 fold greater extracellular Ca^{2+} concentration. In WT and TRPC1$^{-/-}$ Subc AT cells, increasing extracellular

Ca^{2+} to both 2 and 4 fold produced no change in lipid accumulation, however $TRPC1^{-/-}$ adipocytes had significantly less lipid than WT. The increase in extracellular Ca^{2+} concentration by 2- and 4-fold resulted in a decrease in expression of Perilipin, FABP4, and PPARγ in both WT and $TRPC1^{-/-}$ Subc adipocytes. Together this data indicates TRPC1 is an important SOCE channel in Subc AT and loss of TRPC1 results in reduced Ca^{2+} influx and diminished differentiation. Furthermore, extracellular Ca^{2+} concentrations are important in adipogenic protein expression.

Next, VAT from WT and $TRPC1^{-/-}$ mice was evaluated in the same manner as for Subc AT experiments. Electrophysiological recordings of membrane currents indicate TRPC1 currents were significantly reduced in both VAT SVF $TRPC1^{-/-}$ cells (Fig. 5A-C) and differentiated $TRPC1^{-/-}$ VAT (Fig. 5F-H). Interestingly, after differentiation, the Ca^{2+} current in $TRPC1^{-/-}$ VAT was more inwardly rectifying and showed properties similar to ORAI1 currents. Analysis of Ca^{2+} influx upon treatment with Tg showed a decrease in internal ER Ca^{2+} release in $TRPC1^{-/-}$ differentiated VAT adipocytes but not in undifferentiated VAT SVF (Fig. 5D, E, I, J). Similar to Subc AT, addition of external Ca^{2+} resulted in a reduction in Ca^{2+} influx in both types (SVF and differentiated) of $TRPC1^{-/-}$ VAT as compared to WT control. Analysis of lipid accumulation of WT and $TRPC1^{-/-}$ VAT after differentiation revealed a significant reduction in total lipid when TRPC1 is nonfunctional (Fig. 5K, L). This lack of differentiation in $TRPC1^{-/-}$ VAT adipocytes was also evident in the lack of expression of Perilipin, FABP4, and PPARγ (Fig. 5M,N). Notably, increasing extracellular Ca^{2+} concentration during differentiation decreased lipid accumulation when increased by 4-fold in WT VAT, however no change was observed in $TRPC1^{-/-}$ VAT (Fig. 5K, L). When challenged with increased extracellular Ca^{2+} concentrations, expression of Perilipin, FABP4, and PPARγ were progressively decreased in both WT and $TRPC1^{-/-}$ VAT (Fig. 5M,N). Together these results reveal TRPC1 to be a functioning partner in SOCE in not only Subc AT but also VAT. Differentiation in both Subc AT and VAT is inhibited by increased extracellular Ca^{2+}

concentrations, however Subc AT may be less sensitive as shown by total lipid accumulation. Further, differentiation in both tissue types, Subc AT and VAT, is impaired when TRPC1 is nonfunctional.

Serum adipokines levels are reduced in TRPC1$^{-/-}$ mice

Ca^{2+} has been shown in numerous studies to be involved in the secretion of adipokines from AT (Komai et al., 2014; Sukumar et al., 2012; Ye et al., 2010), however the Ca^{2+} channel(s) involved have not been identified. To determine whether the reduction in Ca^{2+} influx in TRPC1$^{-/-}$ AT alters adipokine levels, we assessed serum adiponectin and leptin concentrations of WT and TRPC1$^{-/-}$ mice. Serum concentrations of both adiponectin and leptin were significantly reduced in TRPC1$^{-/-}$ mice aged 3-9 months as compared to their WT age-matched counterpart, with no difference seen at any age group (Fig. 6A, B). There are conflicting views on the effect of a high fat diet on serum adiponectin concentrations (Bullen et al., 2007) leading us next to investigate whether a high fat diet would alter serum adipokine concentrations in TRPC1$^{-/-}$ mice. WT and TRPC1$^{-/-}$ mice were placed on a diet of either normal chow (16% fat) or high fat (45% fat) for 12 weeks and serum adiponectin concentrations were assessed at the end of 12 weeks. Results show a reduction in serum adiponectin concentrations in TRPC1$^{-/-}$ mice fed a normal chow diet when compared to WT, however the high fat diet failed to induce a change in serum adiponectin concentrations in the TRPC1$^{-/-}$ mice (Fig. 6E).

Adiponectin and leptin are almost entirely produced by adipocytes which led us to question whether the reduction in serum concentrations seen in TRPC1$^{-/-}$ mice was due to a decrease in overall production. To access this, Subc AT and VAT lysates from WT and TRPC1$^{-/-}$ mice were evaluated for adiponectin and leptin protein expression. No difference was observed in either adiponectin or leptin expression between AT obtained from TRPC1$^{-/-}$ or their WT counter parts (Fig. 6C, D). Interestingly, both WT and TRPC1$^{-/-}$ VAT samples contained higher levels of both adiponectin and leptin than Subc AT samples possibly indicating VAT may play a larger role as a distributor of adipokines. Overall, these

results suggest that reduced serum adiponectin and leptin concentrations in TRPC1$^{-/-}$ mice are not likely a consequence of lower AT production and TRPC1$^{-/-}$ mice serum adiponectin concentrations are not affected by a high-fat diet.

Adiponectin isoforms are altered in TRPC1$^{-/-}$ mice

Adiponectin is first formed as a 30 kDa monomer that can be assembled within the ER into complex isoforms such as high (HMW), medium (MMW), and low (LMW) molecular weights. The HMW isoform is thought to be the most biologically active and Ca^{2+} is important in its formation (Banga et al., 2008; Rosen and Spiegelman, 2014). Though Ca^{2+} dependency has been shown, the specific Ca^{2+} channel involved has yet to be determined. Evaluation of serum adiponectin from WT and TRPC1$^{-/-}$ mice by non-denaturing gel electrophoresis indicated a significant reduction in both HMW and MMW isoforms with no difference in LMW (Fig. 6F, G). To understand whether the reduction of HMW and MMW isoforms in TRPC1$^{-/-}$ mouse serum is due to an issue in adiponectin production and folding within AT, Subc AT and VAT adiponectin isoform composition was assessed. In all three isoforms, there was no difference observed between WT and TRPC1$^{-/-}$ in either Subc AT or VAT indicating isoform assembly is not a likely candidate for differences in serum levels (Fig. 6H). Within these studies, we observed TRPC1$^{-/-}$ mice have less biologically active adiponectin (HMW) in serum than WT mice, which does not correspond to intracellular tissue quantities.

Reduced SNARE protein interactions in TRPC1$^{-/-}$ adipose tissue

Secretion of adiponectin from AT can be triggered through treatment with insulin. To mimic this process ex vivo, fresh Subc AT from WT and TRPC1$^{-/-}$ mice was cut into 8-15 mg pieces and stimulated with insulin (100 nM) for 6 hours. Upon insulin stimulation, secreted adiponectin concentrations were significantly increased in WT Subc AT compared to non-treated control (Fig. 7A). Importantly, treatment of TRPC1$^{-/-}$ Subc AT with insulin did not result in a significant increase in adiponectin

secretion as seen in the WT Subc AT (Fig 7A, B). Analysis of adiponectin isoforms upon insulin stimulation showed a reduction in HMW secretion (Fig. 7B) with a converse increase in LMW in all tissue types and animals (data not shown). This data indicates adipocytes with TRPC1 deficiency has a reduced response to insulin–stimulated secretion of adiponectin.

Our lab has shown a functional interaction between SNARE family proteins is required for intracellular vesicle fusion and Ca^{2+} influx (Singh et al., 2004). Vesicle-associated membrane protein 2 (VAMP-2) is found within the plasma membrane and intracellular vesicles and is involved in the docking of the vesicles to the plasma membrane by interacting with plasma membrane SNARE proteins, such as syntaxin and SNAP. To assess whether TRPC1 may be involved in SNARE complex formation needed to exocytose adipokine vesicles from AT, co-immunoprecipitation was performed on fresh AT samples. Subc AT and VAT were isolated from WT and $TRPC1^{-/-}$ mice and homogenized, quantified and incubated with insulin (100 nM), SKF (10 μM), or Tg (1 μM) for 30 min. Figures 7C, E show that plasma membrane SNARE components syntaxin 1 and SNAP25 co-immunoprecipitated with VAMP2 in both WT and $TRPC1^{-/-}$ control samples. Upon treatment with insulin, the interaction of VAMP-2 with syntaxin 1 and SNAP25 increased in WT samples, however no change was observed in $TRPC1^{-/-}$. Pretreatment with SKF prior to insulin did not change the effect of insulin on interactions of SNAP25 with VAMP-2 in WT AT, however it did reduce interactions of VAMP-2 with syntaxin 1. Treatment of $TRPC1^{-/-}$ AT cells with SKF had no effect on interactions of either syntaxin-1 or SNAP25 with VAMP-2 (Fig. 7C-F). Raising $[Ca^{2+}]_i$ through treatment with Tg increased SNAP-25 and VAMP-2 interactions in WT AT, however it did not result in a change in WT VAMP-2 and syntaxin 1 interactions or any interactions within $TRPC1^{-/-}$ AT. Together these results indicate insulin stimulated SNARE complex formation in AT involves TRPC1-mediated Ca^{2+} entry, which is needed for exocytosis of adiponectin.

Discussion

The incidence of obesity-associated diseases such as type 2 diabetes, hypertension, cardiovascular risk, and cancer has increased drastically worldwide. Consequently, scientific inquiry into the mechanisms underlying AT development and the pathology of obesity has gained interest. Though an array of metabolic disorders are linked to alterations of Ca^{2+} homeostasis (Arruda and Hotamisligil, 2015), the study of Ca^{2+} within AT has been underrepresented. Evidence suggests AT $[Ca^{2+}]_i$ is partly mediated by SOCE, thus we focused on the identification of the endogenous Ca^{2+} entry channel and establish its role in adipocyte function. In our study, we identify TRPC1 as a major regulator of adipocyte energy metabolism through mediation of adipocyte differentiation and SNARE complex formation needed for adipokine secretion.

SOCE was first identified as a major component of non-excitable cells (Parekh and Putney, 2005), but further research has identified SOCE within a multitude of tissue types. This knowledge has unveiled it to be a ubiquitous Ca^{2+} signaling pathway which regulates numerous cellular functions including those connected with diabetic complications (Chaudhari and Ma, 2016). Identification of SOCE mechanisms within adipocytes may lead to a better understanding of the onset of obesity and metabolic disorders and reveal therapeutic possibilities. Within our study, Ca^{2+} entry was demonstrated to have SOCE properties that could effectively be reduced by the addition of a non-specific Ca^{2+} entry channel blocker SKF in both Subc AT and VAT indicating a similar mechanism for Ca^{2+} entry influx between the tissue types. Furthermore, the current properties observed and blocked by SKF, 2APB and BTP2 were similar to that of TRPC1 channel (Liu et al., 2003; Selvaraj et al., 2012). Upon differentiation, a higher amplitude of TRPC1-like current in both Subc AT and VAT was observed which is most likely attributable to the more than 2-fold upregulation of TRPC1 expression. The role of SOCE and the specific Ca^{2+} channel involved within Subc AT and VAT was further confirmed using adipose tissue with a genetic ablation of TRPC1. Loss of TRPC1 showed a significant decrease in Ca^{2+}

entry upon treatment with Tg in SVF and differentiated adipocytes of both tissue types. In all TRPC1$^{-/-}$ adipose types except differentiated VAT, a decrease in internal ER Ca^{2+} was observed upon treatment with Tg which is most likely attributed to a decrease in ER Ca^{2+} pool. A small ER in TRPC1$^{-/-}$ cells could impair the ability of the ER to synthesize proteins and lipids properly. Importantly, although ORAI1 was present, it was not able to compensate for the loss of TRPC1, suggesting that the major Ca^{2+} entry channel in adipocytes is mediated via TRPC1. TRPC5 expression is increased upon adipocytes differentiation; however as TRPC1 forms C1/C5 heterotetramers (Shi et al., 2012), loss of TRPC1 would inactivate TRPC5 and thus could not compensate in TRPC1$^{-/-}$ mice.

Adipocyte differentiation is a complex process and dysregulation can lead to lipid accumulation and altered energy and metabolic regulation. Though the process is not fully understood, several studies have identified Ca^{2+} dependency within adipocyte differentiation (Jensen et al., 2004; Neal and Clipstone, 2002; Pramme-Steinwachs et al., 2017; Shi et al., 2000). Our studies are the first to use both genetic and pharmacological inhibitors to show that Ca^{2+} entry via TRPC1 is essential for adipocyte differentiation. Use of SKF to block store-mediated Ca^{2+} entry during differentiation not only impaired lipid droplet formation in WT Subc AT and VAT SVF, but also inhibited the expression of lipid mobilization proteins FABP4 and Perilipin. The transcription factor PPARγ is essentially expressed during early differentiation stages and regulates a number of adipocyte marker genes, including FABP4 and perilipin (Farmer, 2006; Wu et al., 1999). Here we show blockage of Ca^{2+} influx by SKF suppresses PPARγ expression indicating Subc AT and VAT SVF may be unable to induce the initial processes of differentiation when SOCE is inhibited. Suppression of SOCE by TRPC1 loss, as seen in TRPC1$^{-/-}$ Subc and VAT cells, resulted in a reduction but not a complete impairment of lipid accumulation in both tissue types. Correspondingly, TRPC1$^{-/-}$ Subc and VAT differentiated adipocyte expression of FABP4, perilipin, and PPARγ was reduced when compared to WT indicating TRPC1 may be involved in the initial stages of PPARγ mediated differentiation. TRPC1 channels are also activated

by GPCRs that induces the production of second messenger IP3, which bonds to IP3R in the ER thereby leading to store depletion. Recently several GPCRs have been identified in adipocyte cells (Klepac et al., 2016). For example Endothelin (ET) receptors type A and B (*Ednra* and *Ednrb*), Adrenoceptor Alpha 1A (*Adra1a*), Angiotensin II receptor, type 1a and 1b (*Agtr1a* and *Agtr1b*) and Cholinergic Receptor, Muscarinic 3 (*Chrm3*). Importantly, an increase in the expression of *GPCRs* was also observed during differentiation, which further supports our data and an increase in Ca^{2+} entry was observed in differentiated cells. In addition, insulin receptor signaling could also be involved. Binding of insulin to its receptor has been shown to inhibit SERCA thus increasing cytosolic Ca^{2+} levels (Borge et al., 2002) and thus could also play a role in the activation of TRPC1 channels.

In contrast to Ca^{2+} blockage, continuous exposure to high external Ca^{2+} has been shown to inhibit preadipocyte differentiation (Jensen et al., 2004) and block adipocyte lipid accumulation and expression of adipogenic transcription factors (Pramme-Steinwachs et al., 2017; Shi et al., 2000). Within our study, increasing extracellular Ca^{2+} concentrations by 4-fold decreased differentiation in WT VAT but had no effect on Subc AT. Interestingly, a slight difference in lipid accumulation was observed between WT Subc AT and WT VAT at all Ca^{2+} concentrations. Subc AT is known to have greater differentiation potential and proliferative ability when compared to VAT (Baglioni et al., 2012), which most likely explains the differences observed in WT Subc and VAT lipid accumulations. Subc AT was able to overcome the inhibitory effect of the increased extracellular Ca^{2+} to sustain lipid accumulation whereas VAT adipocytes were not. Though increasing extracellular Ca^{2+} concentrations had no effect on lipid accumulation in Subc AT, protein expression of key differentiation factors reduced when Ca^{2+} increased which is similar to that of VAT. This may confirm what other studies have shown that extended exposure to high Ca^{2+} concentrations inhibits differentiation of adipocytes, particularly in VAT. In addition, current properties in differentiated VAT cells, especially in $TRPC1^{-/-}$, were similar to that observed with ORAI1. This suggests that ORAI1 could play a role in

VAT tissues, however further research is needed to fully establish the role of ORAI1 in these cells; nonetheless ORAI1 was not able to compensate for the loss of TRPC1.

Impaired adipogenesis can lead to a multitude of different outcomes with the most common being an unhealthy expansion of adipose tissue. This phenomenon is generally seen in adult obesity which is hypertrophic in nature and the reason why PPARγ agonists such as TZDs are useful in obesity (Choe et al., 2016). Within our study, TRPC1$^{-/-}$ mice exhibited increased adipose tissue accumulation as they aged; however overall body weight did not significantly increase relative to WT mice. This increase in adipose accumulation could be due to dysfunctional adipose differentiation and/or induction of lipogenesis which in time results in a hypertrophic expansion. Another important finding was that organ weights were reduced, which could be due to the fact that TRPC1 has been shown to play a critical role in cell proliferation(Alonso-Carbajo et al., 2017) and be a reason for the increase in adipose accumulation without an increase in body weight. TRPC1$^{-/-}$ mice could also have reduced lipolysis. If this is the case, fatty acids are not mobilized from triacylglycerol stores properly, which in turn would expand adipose tissue volume over time. Furthermore, deletion of FABP4 has been shown to reduce lipolysis and FABP4 knockout mice have increased white AT mass on a high fat diet (Hotamisligil et al., 1996). In our model, lack of TRPC1 may inhibit the expression FABP4 thus reducing lipolysis. Another possibility is that TRPC1 could be involved in store-operated Ca^{2+} entry necessary to induce lipolysis. Lack of store-operated Ca^{2+} entry proteins, have shown to disrupt regulators of lipid metabolism and results in increased organ lipid droplet formation (Maus et al., 2017). Together, these results indicate that SOCE via TRPC1 may be involved in the initial stages of adipocyte differentiation of both Subc AT and VAT and result in increased adipose tissue volume over time, however more research needs to be done to determine the exact mechanism.

Reduced secretion of adiponectin resulting in low serum concentrations is a common feature of obesity (Kovacova et al., 2012), whereas low serum leptin is used as an indicator of malnutrition (Amirkalali et al., 2010). TRPC1$^{-/-}$ mice present both reduced serum adiponectin and leptin concentrations, however TRPC1$^{-/-}$ mice do not display either of these phenotypes. Food consumption and weight measurements of TRPC1$^{-/-}$ mice were similar to WT throughout their lifetime, however as they age their volume of adipose deposits increases. This increase in adiposity later in life is most likely due to suppressed adiponectin secretion which lowers overall body metabolism and possible lipolysis dysfunction (Figure 7G). Importantly, equal concentrations of adiponectin and leptin were observed within the Subc AT and VAT samples of WT and TRPC1$^{-/-}$ mice, which is contrary to the reduced serum concentrations in TRPC1$^{-/-}$ mice. This indicates that there is no reduction in adipokine production, but rather the release of adipokines is affected in TRPC1$^{-/-}$ mice. Interestingly, the greatest reduction in serum adiponectin in obese subjects is from Subc AT and the metabolically active isoform HMW (Kovacova et al., 2012). Analysis of serum adiponectin isoforms in our study indicates a similar reduction in HMW secretion, however internal AT concentrations of adiponectin were similar between WT and TRPC1$^{-/-}$. This reduction in TRPC1$^{-/-}$ serum HMW isoform is most likely due to increased utilization by downstream targets, such as muscle and liver, since overall abundance is diminished. However, another caveat is that these are global TRPC1KOs that might affect additional system and caution should be used in the interpretation of the data. To understand the mechanisms as how TRPC1 regulate adipokine secretion, we provide evidence that insulin stimulated TRPC1 mediated Ca^{2+} influx is necessary for fusion of VAMP-2 with SNAP25 and syntaxin1, thus necessary for the secretion of adipokines. Thus, overall, our results provide evidence that TRPC1 not only plays a key role in adipocytes differentiation, but is essential for adipokine secretion, and dysfunction in these vital processes would lead to obesity and metabolic syndrome.

Methods

Animals

Male B6129SF2/J (WT) or TRPC1 knockout ($TRPC1^{-/-}$ in the same background) mice (Jackson Laboratories, Bar Harbor, MI) were used for these experiments. All animals were housed in a temperature controlled room under a 12/12 h light/dark cycle with ad libitum access to food and water. All animal experiments were carried out as per the institutional guidelines for the use and care of animals. For high-fat diet experimentation, four month old males were fed diets containing either 16% (normal-fat, NF) or 45% fat (high-fat, HF) for 12 weeks. All animal protocols were approved by the institutional IACUC committee.

Cell culture and Cell Cycle analysis

Subcutaneous and visceral adipose tissue was digested and SVF fraction was isolated for culture and differentiation as previously described (Claycombe et al., 2016; Harkins et al., 2004). Cell cycle analysis was performed by staining the DNA with fluorescent dye (propidium iodide 50 ug/mL overnight) and data was analyzed using a flow cytometer.

Calcium imaging

Cells were incubated with 2uM Fura-2 (Molecular Probes) and the fluorescence intensity was monitored with a CCD camera-based imaging system (Compix) mounted on an Olympus XL70 inverted microscope equipped with an Olympus 40× (1.3 NA) objective. A dual wavelength monochromator enabled alternative excitation at 340 and 380 nm, whereas the emission fluorescence was monitored at 510 nm with an Orca Imaging camera (Hamamatsu, Japan). Fluorescence traces shown represent $[Ca^{2}+]_i$ values in 340/380 nm ratio that are a representative of results obtained in at least 3-4 individual experiments using 40-70 cells in each experiment.

Immunoblotting and Co-immunoblotting

Crude lysates were prepared from Subc AT and VAT and SVF and differentiated adipocyte cultures. Protein was resolved on NuPAGE Novex 4-12% Bis-Tris gels, transferred to nitrocellulose membranes and probed with respective antibodies. Densitometric analysis was performed using image J analysis and results were corrected for protein loading by normalization to β-actin levels. Non-denaturing PAGE was performed by resolving protein in Novex Tris-Glycine Native Sample Buffer on NuPAGE™ 3-8% Tris-Acetate Protein Gels. For the co-IP assays, Subc AT and VAT was manually homogenized in the presence of HBSS containing Ca^{2+} and Mg^{2+} and then treated as described for 30 min at 37°C. Samples were incubated overnight with anti-VAMP2 antibody after which agarose anti-mouse IgG beads were added. Isolated beads were then washed, boiled, and separated by SDS-PAGE. SNARE proteins were detected using the indicated antibodies.

EchoMRI measurements of body composition

Whole body composition, including fat mass and lean mass, was determined using nuclear magnetic resonance technology with the EchoMRI700™ instrument (Echo Medical Systems, Houston, TX).

Red Oil Staining

Culture plates were washed by PBS and cells were fixed in 4% formalin, followed by staining with oil-red-O (Sigma) and photographed. The dye was then extracted with 100% isopropanol and the absorbance was determined at 492 nm.

Elisa

Serum, culture media, and protein lysates samples were analyzed for adiponectin and leptin using an adiponectin Mouse ELISA kit (Abcam) and Leptin Mouse ELISA kit (Invitrogen).

Electrophysiology

For patch clamp experiments, coverslips with cells were transferred to the recording chamber and perfused with an external Ringer's solution using previous protocol (Sukumaran et al., 2015). Whole cell currents were recorded using an Axopatch 200B (Axon Instruments, Inc.). The patch pipette had resistances between 3 -5 MΩ after filling with the standard intracellular solution that contained the following (mM): cesium methane sulfonate, 150; NaCl, 8; Hepes, 10; EGTA, 10; pH 7.2 (CsOH). Basal leak was subtracted from the final currents and average currents are shown. The maximum peak currents were calculated at a holding potential of –80 mV. The voltage-current (I-V) curves were made using a ramp protocol ranging from -100mV to +100mV and 100ms duration were delivered at 2s intervals, whereby current density was evaluated at various membrane potentials and plotted.

PCR analysis

Total RNA was extracted using the RNeasy Lipid Tissue Mini kit and Qiacube (Qiagen, Valencia, CA) from flash-frozen subcutaneous adipose tissue. cDNA was synthesized using the Quantitect Reverse Transcriptase kit (Qiagen, Valencia, CA) Rox FastStart Universal Probe Master mix assay reagents were purchased from Roche (Indianapolis, IN). Primers were purchased from Integrated DNA Technology (IDT, Coralville, IA). The endogenous control (18S rRNA) was purchased from Applied Biosystems (Foster City, CA). RT-PCR analysis for TRPC1 transcripts was done with primers from the eighth and ninth exons (Up-5' GCAACCTTTGCCCTCAAAGTG and Dn-5' GGAGGAACATT-CCCAGAAATTTCC) after the EcoRI site (Eurofins MWG Operon, Huntsville, AL).

Statistical Analysis

Mean and standard error values were computed for all continuous variables and frequency distributions were calculated for all categorical variables. Statistical comparisons were made using Student's t test or ANOVA. When an interaction was significant ($p < 0.05$), Tukey contrasts were used

to perform pairwise comparisons. All statistical tests were two-tailed with significant reported as follows: *, $p < 0.05$; **, $p < 0.01$; ***, $p < 0.001$; ****, $p < 0.0001$.

Acknowledgements

We thank Dr. Nascimento for the cell cycle analysis. This work was funded by grant support from the National Institutes of Health (R01DE017102; R01 DE022765) awarded to B.B.S., the ND EPSCoR through National Science Foundation (IIA-1355466) awarded to A.E.S., the USDA Agricultural Research Service Project #3062-51000-052-00D awarded to K.J.L and and Z01-636 ES-101684 to LB). The funders (NIH/USDA) had no further role in study design, data analysis, and/or interpretation of the data.

Author Contributions

Conceptualization, Methodology, and Formal Analysis, B.B.S. and A.S; Investigation, D.K., A.S., Y.S., P.S., and T.R; Resources, B.B.S. and L.B. (developed TRPC1$^{-/-}$ mice); Writing–Original Draft, A.S., B.B.S., and K.J.C.-L; Writing–Review and Editing, L.B., T.R., and J.N.R.; Visualization, B.B.S. and A.S.; Supervision, B.B.S., J.N.R., K.J.C-L.

Declaration of Interests

The authors declare no conflict of interest.

References

Alonso-Carbajo, L., Kecskes, M., Jacobs, G., Pironet, A., Syam, N., Talavera, K. and Vennekens, R. (2017). Muscling in on TRP channels in vascular smooth muscle cells and cardiomyocytes. *Cell Calcium* **66**, 48-61.

Amirkalali, B., Sharifi, F., Fakhrzadeh, H., Mirarefein, M., Ghaderpanahi, M., Badamchizadeh, Z. and Larijani, B. (2010). Low serum leptin serves as a biomarker of malnutrition in elderly patients. *Nutr Res* **30**, 314-9.

Arita, Y., Kihara, S., Ouchi, N., Takahashi, M., Maeda, K., Miyagawa, J., Hotta, K., Shimomura, I., Nakamura, T., Miyaoka, K. et al. (1999). Paradoxical decrease of an adipose-specific protein, adiponectin, in obesity. *Biochem Biophys Res Commun* **257**, 79-83.

Arruda, A. P. and Hotamisligil, G. S. (2015). Calcium Homeostasis and Organelle Function in the Pathogenesis of Obesity and Diabetes. *Cell Metab* **22**, 381-97.

Asanov, A., Sampieri, A., Moreno, C., Pacheco, J., Salgado, A., Sherry, R. and Vaca, L. (2015). Combined single channel and single molecule detection identifies subunit composition of STIM1-activated transient receptor potential canonical (TRPC) channels. *Cell Calcium* **57**, 1-13.

Baglioni, S., Cantini, G., Poli, G., Francalanci, M., Squecco, R., Di Franco, A., Borgogni, E., Frontera, S., Nesi, G., Liotta, F. et al. (2012). Functional differences in visceral and subcutaneous fat pads originate from differences in the adipose stem cell. *PLoS One* **7**, e36569.

Banga, A., Bodles, A. M., Rasouli, N., Ranganathan, G., Kern, P. A. and Owens, R. J. (2008). Calcium is involved in formation of high molecular weight adiponectin. *Metab Syndr Relat Disord* **6**, 103-11.

Berridge, M. J., Lipp, P. and Bootman, M. D. (2000). The versatility and universality of calcium signalling. *Nat Rev Mol Cell Biol* **1**, 11-21.

Birnbaumer, L., Zhu, X., Jiang, M., Boulay, G., Peyton, M., Vannier, B., Brown, D., Platano, D., Sadeghi, H., Stefani, E. et al. (1996). On the molecular basis and regulation of cellular capacitative calcium entry: roles for Trp proteins. *Proc Natl Acad Sci U S A* **93**, 15195-202.

Bogan, J. S. and Lodish, H. F. (1999). Two compartments for insulin-stimulated exocytosis in 3T3-L1 adipocytes defined by endogenous ACRP30 and GLUT4. *J Cell Biol* **146**, 609-20.

Borge, P. D., Moibi, J., Greene, S. R., Trucco, M., Young, R. A., Gao, Z. and Wolf, B. A. (2002). Insulin receptor signaling and sarco/endoplasmic reticulum calcium ATPase in beta-cells. *Diabetes* **51 Suppl 3**, S427-33.

Brose, N., Petrenko, A. G., Südhof, T. C. and Jahn, R. (1992). Synaptotagmin: a calcium sensor on the synaptic vesicle surface. *Science* **256**, 1021-5.

Bullen, J. W., Bluher, S., Kelesidis, T. and Mantzoros, C. S. (2007). Regulation of adiponectin and its receptors in response to development of diet-induced obesity in mice. *Am J Physiol Endocrinol Metab* **292**, E1079-86.

Catterall, W. A. (2000). Structure and regulation of voltage-gated Ca2+ channels. *Annu Rev Cell Dev Biol* **16**, 521-55.

Chaudhari, S. and Ma, R. (2016). Store-operated calcium entry and diabetic complications. *Exp Biol Med (Maywood)* **241**, 343-52.

Choe, S. S., Huh, J. Y., Hwang, I. J., Kim, J. I. and Kim, J. B. (2016). Adipose Tissue Remodeling: Its Role in Energy Metabolism and Metabolic Disorders. *Front Endocrinol (Lausanne)* **7**, 30.

Claycombe, K. J., Vomhof-DeKrey, E. E., Garcia, R., Johnson, W. T., Uthus, E. and Roemmich, J. N. (2016). Decreased beige adipocyte number and mitochondrial respiration

coincide with increased histone methyl transferase (G9a) and reduced FGF21 gene expression in Sprague-Dawley rats fed prenatal low protein and postnatal high-fat diets. *J Nutr Biochem* **31**, 113-21.
Cong, L., Chen, K., Li, J., Gao, P., Li, Q., Mi, S., Wu, X. and Zhao, A. Z. (2007). Regulation of adiponectin and leptin secretion and expression by insulin through a PI3K-PDE3B dependent mechanism in rat primary adipocytes. *Biochem J* **403**, 519-25.
Fabbrini, E., Sullivan, S. and Klein, S. (2010). Obesity and nonalcoholic fatty liver disease: biochemical, metabolic, and clinical implications. *Hepatology* **51**, 679-89.
Farmer, S. R. (2006). Transcriptional control of adipocyte formation. *Cell Metab* **4**, 263-73.
Feske, S., Gwack, Y., Prakriya, M., Srikanth, S., Puppel, S. H., Tanasa, B., Hogan, P. G., Lewis, R. S., Daly, M. and Rao, A. (2006). A mutation in Orai1 causes immune deficiency by abrogating CRAC channel function. *Nature* **441**, 179-85.
Foster, M. T., Shi, H., Softic, S., Kohli, R., Seeley, R. J. and Woods, S. C. (2011). Transplantation of non-visceral fat to the visceral cavity improves glucose tolerance in mice: investigation of hepatic lipids and insulin sensitivity. *Diabetologia* **54**, 2890-9.
Fruebis, J., Tsao, T. S., Javorschi, S., Ebbets-Reed, D., Erickson, M. R., Yen, F. T., Bihain, B. E. and Lodish, H. F. (2001). Proteolytic cleavage product of 30-kDa adipocyte complement-related protein increases fatty acid oxidation in muscle and causes weight loss in mice. *Proc Natl Acad Sci U S A* **98**, 2005-10.
Graham, S. J., Black, M. J., Soboloff, J., Gill, D. L., Dziadek, M. A. and Johnstone, L. S. (2009). Stim1, an endoplasmic reticulum Ca2+ sensor, negatively regulates 3T3-L1 pre-adipocyte differentiation. *Differentiation* **77**, 239-47.
Haider, N., Dusseault, J., Rudich, A. and Larose, L. (2017). Nck2, an unexpected regulator of adipogenesis. *Adipocyte* **6**, 154-160.
Harkins, J. M., Moustaid-Moussa, N., Chung, Y. J., Penner, K. M., Pestka, J. J., North, C. M. and Claycombe, K. J. (2004). Expression of interleukin-6 is greater in preadipocytes than in adipocytes of 3T3-L1 cells and C57BL/6J and ob/ob mice. *J Nutr* **134**, 2673-7.
Hotamisligil, G. S., Johnson, R. S., Distel, R. J., Ellis, R., Papaioannou, V. E. and Spiegelman, B. M. (1996). Uncoupling of obesity from insulin resistance through a targeted mutation in aP2, the adipocyte fatty acid binding protein. *Science* **274**, 1377-9.
Hui, X., Gu, P., Zhang, J., Nie, T., Pan, Y., Wu, D., Feng, T., Zhong, C., Wang, Y., Lam, K. S. et al. (2015). Adiponectin Enhances Cold-Induced Browning of Subcutaneous Adipose Tissue via Promoting M2 Macrophage Proliferation. *Cell metabolism* **22**, 279-90.
Ibrahim, M. M. (2010). Subcutaneous and visceral adipose tissue: structural and functional differences. *Obes Rev* **11**, 11-8.
Isakson, P., Hammarstedt, A., Gustafson, B. and Smith, U. (2009). Impaired preadipocyte differentiation in human abdominal obesity: role of Wnt, tumor necrosis factor-alpha, and inflammation. *Diabetes* **58**, 1550-7.
Jensen, B., Farach-Carson, M. C., Kenaley, E. and Akanbi, K. A. (2004). High extracellular calcium attenuates adipogenesis in 3T3-L1 preadipocytes. *Exp Cell Res* **301**, 280-92.
Kadiri, S., Auclair, M., Capeau, J. and Antoine, B. (2017). Depot-Specific Response of Adipose Tissue to Diet-Induced Inflammation: The Retinoid-Related Orphan Receptor α (RORα) Involved? *Obesity (Silver Spring)* **25**, 1948-1955.
Kim, S. M., Lun, M., Wang, M., Senyo, S. E., Guillermier, C., Patwari, P. and Steinhauser, M. L. (2014). Loss of white adipose hyperplastic potential is associated with enhanced susceptibility to insulin resistance. *Cell Metab* **20**, 1049-58.
Klepac, K., Kilić, A., Gnad, T., Brown, L. M., Herrmann, B., Wilderman, A., Balkow, A., Glöde, A., Simon, K., Lidell, M. E. et al. (2016). The Gq signalling pathway inhibits brown and beige adipose tissue. *Nat Commun* **7**, 10895.

Komai, A. M., Brännmark, C., Musovic, S. and Olofsson, C. S. (2014). PKA-independent cAMP stimulation of white adipocyte exocytosis and adipokine secretion: modulations by Ca2+ and ATP. *J Physiol* **592**, 5169-86.
Kovacova, Z., Tencerova, M., Roussel, B., Wedellova, Z., Rossmeislova, L., Langin, D., Polak, J. and Stich, V. (2012). The impact of obesity on secretion of adiponectin multimeric isoforms differs in visceral and subcutaneous adipose tissue. *Int J Obes (Lond)* **36**, 1360-5.
Lehr, S., Hartwig, S. and Sell, H. (2012). Adipokines: a treasure trove for the discovery of biomarkers for metabolic disorders. *Proteomics Clin Appl* **6**, 91-101.
Liao, Y., Erxleben, C., Abramowitz, J., Flockerzi, V., Zhu, M. X., Armstrong, D. L. and Birnbaumer, L. (2008). Functional interactions among Orai1, TRPCs, and STIM1 suggest a STIM-regulated heteromeric Orai/TRPC model for SOCE/Icrac channels. *Proc Natl Acad Sci U S A* **105**, 2895-900.
Liu, X., Groschner, K. and Ambudkar, I. S. (2004). Distinct Ca(2+)-permeable cation currents are activated by internal Ca(2+)-store depletion in RBL-2H3 cells and human salivary gland cells, HSG and HSY. *J Membr Biol* **200**, 93-104.
Liu, X., Singh, B. B. and Ambudkar, I. S. (2003). TRPC1 is required for functional store-operated Ca2+ channels. Role of acidic amino acid residues in the S5-S6 region. *J Biol Chem* **278**, 11337-43.
MacDougald, O. A. and Burant, C. F. (2007). The rapidly expanding family of adipokines. *Cell Metab* **6**, 159-61.
Matsuzawa, Y. (2010). Establishment of a concept of visceral fat syndrome and discovery of adiponectin. *Proc Jpn Acad Ser B Phys Biol Sci* **86**, 131-41.
Maus, M., Cuk, M., Patel, B., Lian, J., Ouimet, M., Kaufmann, U., Yang, J., Horvath, R., Hornig-Do, H. T., Chrzanowska-Lightowlers, Z. M. et al. (2017). Store-Operated Ca(2+) Entry Controls Induction of Lipolysis and the Transcriptional Reprogramming to Lipid Metabolism. *Cell Metab* **25**, 698-712.
Neal, J. W. and Clipstone, N. A. (2002). Calcineurin mediates the calcium-dependent inhibition of adipocyte differentiation in 3T3-L1 cells. *J Biol Chem* **277**, 49776-81.
O'Rourke, R. W., Metcalf, M. D., White, A. E., Madala, A., Winters, B. R., Maizlin, I. I., Jobe, B. A., Roberts, C. T., Slifka, M. K. and Marks, D. L. (2009). Depot-specific differences in inflammatory mediators and a role for NK cells and IFN-gamma in inflammation in human adipose tissue. *Int J Obes (Lond)* **33**, 978-90.
Okada-Iwabu, M., Yamauchi, T., Iwabu, M., Honma, T., Hamagami, K., Matsuda, K., Yamaguchi, M., Tanabe, H., Kimura-Someya, T., Shirouzu, M. et al. (2013). A small-molecule AdipoR agonist for type 2 diabetes and short life in obesity. *Nature* **503**, 493-9.
Ouchi, N., Parker, J. L., Lugus, J. J. and Walsh, K. (2011). Adipokines in inflammation and metabolic disease. *Nat Rev Immunol* **11**, 85-97.
Parekh, A. B. and Putney, J. W. (2005). Store-operated calcium channels. *Physiol Rev* **85**, 757-810.
Pramme-Steinwachs, I., Jastroch, M. and Ussar, S. (2017). Extracellular calcium modulates brown adipocyte differentiation and identity. *Sci Rep* **7**, 8888.
Putney, J. W., Steinckwich-Besançon, N., Numaga-Tomita, T., Davis, F. M., Desai, P. N., D'Agostin, D. M., Wu, S. and Bird, G. S. (2017). The functions of store-operated calcium channels. *Biochim Biophys Acta* **1864**, 900-906.
Rasouli, N. and Kern, P. A. (2008). Adipocytokines and the metabolic complications of obesity. *J Clin Endocrinol Metab* **93**, S64-73.
Rosen, E. D. and Spiegelman, B. M. (2006). Adipocytes as regulators of energy balance and glucose homeostasis. *Nature* **444**, 847-53.

Rosen, E. D. and Spiegelman, B. M. (2014). What we talk about when we talk about fat. *Cell* **156**, 20-44.
Seale, P., Conroe, H. M., Estall, J., Kajimura, S., Frontini, A., Ishibashi, J., Cohen, P., Cinti, S. and Spiegelman, B. M. (2011). Prdm16 determines the thermogenic program of subcutaneous white adipose tissue in mice. *J Clin Invest* **121**, 96-105.
Selvaraj, S., Sun, Y., Watt, J. A., Wang, S., Lei, S., Birnbaumer, L. and Singh, B. B. (2012). Neurotoxin-induced ER stress in mouse dopaminergic neurons involves downregulation of TRPC1 and inhibition of AKT/mTOR signaling. *J Clin Invest* **122**, 1354-67.
Shi, H., Halvorsen, Y. D., Ellis, P. N., Wilkison, W. O. and Zemel, M. B. (2000). Role of intracellular calcium in human adipocyte differentiation. *Physiol Genomics* **3**, 75-82.
Shi, J., Ju, M., Abramowitz, J., Large, W. A., Birnbaumer, L. and Albert, A. P. (2012). TRPC1 proteins confer PKC and phosphoinositol activation on native heteromeric TRPC1/C5 channels in vascular smooth muscle: comparative study of wild-type and TRPC1-/- mice. *FASEB J* **26**, 409-19.
Singh, B. B., Lockwich, T. P., Bandyopadhyay, B. C., Liu, X., Bollimuntha, S., Brazer, S. C., Combs, C., Das, S., Leenders, A. G., Sheng, Z. H. et al. (2004). VAMP2-dependent exocytosis regulates plasma membrane insertion of TRPC3 channels and contributes to agonist-stimulated Ca2+ influx. *Mol Cell* **15**, 635-46.
Stern, J. H., Rutkowski, J. M. and Scherer, P. E. (2016). Adiponectin, Leptin, and Fatty Acids in the Maintenance of Metabolic Homeostasis through Adipose Tissue Crosstalk. *Cell Metab* **23**, 770-84.
Sukumar, P., Sedo, A., Li, J., Wilson, L. A., O'Regan, D., Lippiat, J. D., Porter, K. E., Kearney, M. T., Ainscough, J. F. and Beech, D. J. (2012). Constitutively active TRPC channels of adipocytes confer a mechanism for sensing dietary fatty acids and regulating adiponectin. *Circ Res* **111**, 191-200.
Sukumaran, P., Sun, Y., Vyas, M. and Singh, B. B. (2015). TRPC1-mediated Ca^{2+} entry is essential for the regulation of hypoxia and nutrient depletion-dependent autophagy. *Cell Death Dis* **6**, e1674.
Sun, X. and Zemel, M. B. (2007). Calcium and 1,25-dihydroxyvitamin D3 regulation of adipokine expression. *Obesity (Silver Spring)* **15**, 340-8.
Tchoukalova, Y., Koutsari, C. and Jensen, M. (2007). Committed subcutaneous preadipocytes are reduced in human obesity. *Diabetologia* **50**, 151-7.
Thörne, A., Lönnqvist, F., Apelman, J., Hellers, G. and Arner, P. (2002). A pilot study of long-term effects of a novel obesity treatment: omentectomy in connection with adjustable gastric banding. *Int J Obes Relat Metab Disord* **26**, 193-9.
Wu, Z., Rosen, E. D., Brun, R., Hauser, S., Adelmant, G., Troy, A. E., McKeon, C., Darlington, G. J. and Spiegelman, B. M. (1999). Cross-regulation of C/EBP alpha and PPAR gamma controls the transcriptional pathway of adipogenesis and insulin sensitivity. *Mol Cell* **3**, 151-8.
Xie, L., O'Reilly, C. P., Chapes, S. K. and Mora, S. (2008). Adiponectin and leptin are secreted through distinct trafficking pathways in adipocytes. *Biochim Biophys Acta* **1782**, 99-108.
Yamauchi, T., Kamon, J., Waki, H., Terauchi, Y., Kubota, N., Hara, K., Mori, Y., Ide, T., Murakami, K., Tsuboyama-Kasaoka, N. et al. (2001). The fat-derived hormone adiponectin reverses insulin resistance associated with both lipoatrophy and obesity. *Nature medicine* **7**, 941-6.
Ye, F., Than, A., Zhao, Y., Goh, K. H. and Chen, P. (2010). Vesicular storage, vesicle trafficking, and secretion of leptin and resistin: the similarities, differences, and interplays. *J Endocrinol* **206**, 27-36.

Yuan, J. P., Zeng, W., Huang, G. N., Worley, P. F. and Muallem, S. (2007). STIM1 heteromultimerizes TRPC channels to determine their function as store-operated channels. *Nat Cell Biol* **9**, 636-45.
Zhou, H. R., Kim, E. K., Kim, H. and Claycombe, K. J. (2007). Obesity-associated mouse adipose stem cell secretion of monocyte chemotactic protein-1. *Am J Physiol Endocrinol Metab* **293**, E1153-8.

Figures

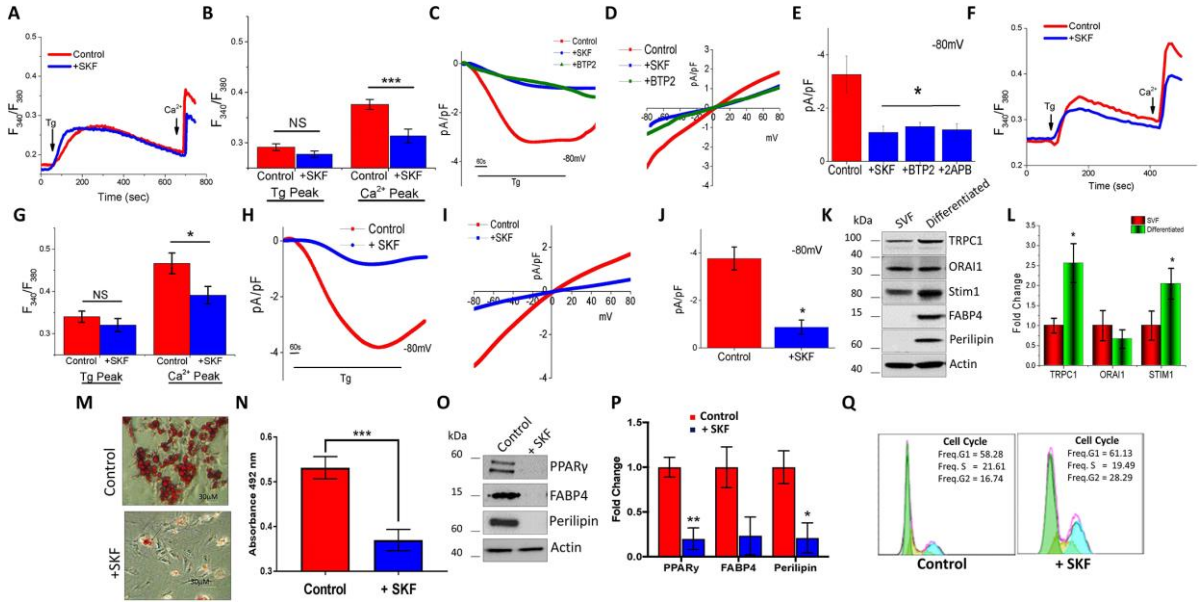

Figure 1: SOCE is essential for the differentiation of subcutaneous adipocytes.

Fura-2 traces of transient increase in $[Ca^{2+}]_i$ after addition of 1 µM Tg and 1 mM Ca^{2+} to Subc AT SVF (A) and differentiated Subc AT (F) in control and cells pretreated with 10 µM SKF for 15 min. Graph quantifies Tg-induced ER Ca^{2+} release and Ca^{2+} entry peaks for Subc AT SVF cells (B) and differentiated Subc AT (G). Each bar gives the mean ± SEM of 60–90 cells in three separate experiments. Application of 1 µM Tg induced inward currents at −80mV in control, SKF, 2APB or BTP- treated Subc AT SVF cells (C) and differentiated Subc AT (H). Respective IV curves are shown for Subc AT SVF (D) and differentiated Subc AT (I). Quantification (n = 7-9 recordings) of current intensity at −80 mV is shown for Subc AT SVF (E) and differentiated Subc AT (J). (K) Western blot with quantification (L) of TRPC1, ORAI1, Stim1, FAPB4, and Perilipin protein expression normalized to actin of Subc AT SVF and differentiated Subc AT (n=3). (M) Oil-red-o staining (using 10X objective) of Subc AT differentiated in the presence of SKF (10 µM) for 7 days. (N) Quantification of absorbance at 492nm of stained lipid droplets using eluted oil-red-o stain (n=3). (O) Western blot of PPARγ, FAPB4, and Perilipin protein expression of Subc AT differentiated in control and in the presence of SKF, quantification in (P) (n=3-4). Q, shows cell cycle analysis on control and SKF treated Subc AT cells (10uM). Graphs are mean ± SEM, significance: *, $p < 0.05$; ***, $p < 0.001$ using ANOVA.

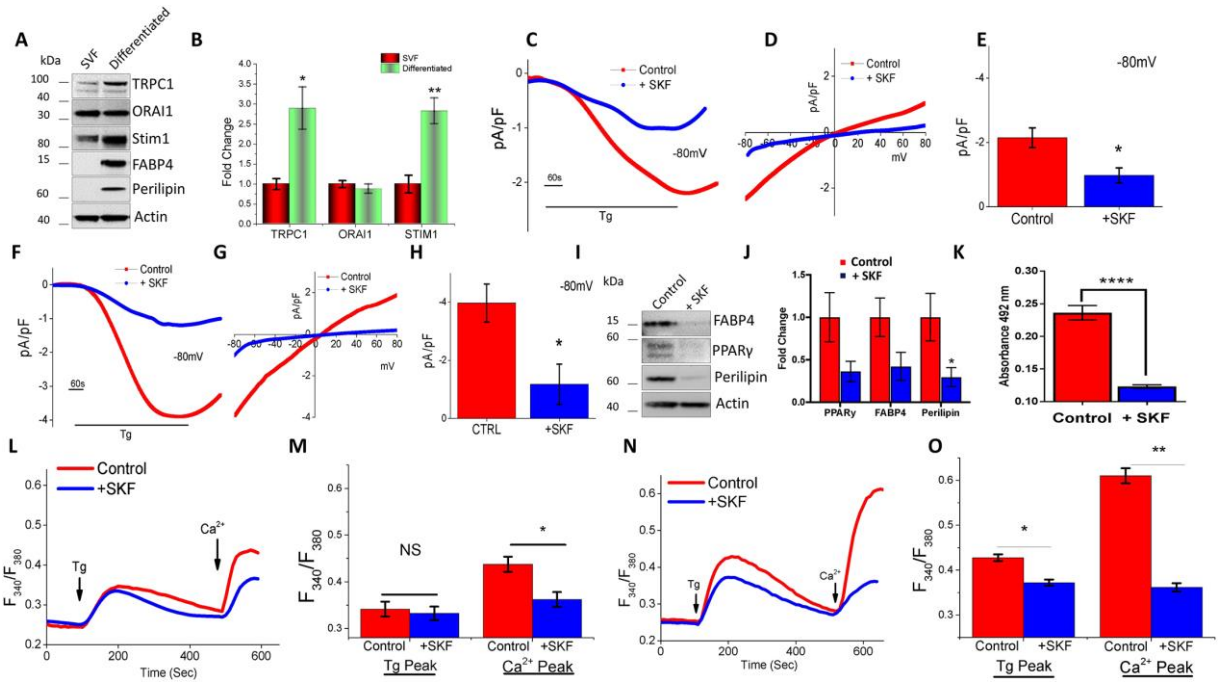

Figure 2: Differentiated visceral adipocytes also exhibit increase in SOCE.

(A) Western blots of TRPC1, ORAI1, Stim1, FAPB4, and Perilipin, and actin protein expression, quantification normalized to actin provided as bar graph in (B), of VAT SVF and differentiated VAT (n=3). Application of 1 μM Tg induced inward currents at −80mV in control and SKF treated VAT SVF cells (C) and differentiated VAT (F). Respective IV curves are shown for VAT SVF (D) and differentiated VAT (G). Quantitation (n = 6 recordings) of current intensity at −80 mV for VAT SVF (E) and differentiated VAT (H). (I) Western blot of PPARγ, FAPB4, and Perilipin protein expression of differentiated VAT treated with SKF with quantification in (J) (n=3-4). (K) Quantification of eluted oil-red-o stain at 492nm of VAT differentiated in the presence of SKF (10 μM) for 7 days (n=3). Fura-2 traces of transient increase in $[Ca^{2+}]_i$ after addition of 1 μM Tg and 1 mM Ca^{2+} to VAT SVF cells (L) and differentiated VAT (N) pretreated with 10 μM SKF for 15 min. Quantification of Tg and Ca^{2+} peaks for VAT SVF cells (M) and differentiated VAT (O). Each bar gives the mean ± SEM of 40–60 cells in three separate experiments. Graphs are mean ± SEM, significance: *, $p < 0.05$; **, $p < 0.01$; ****, $p< 0.0001$ using ANOVA.

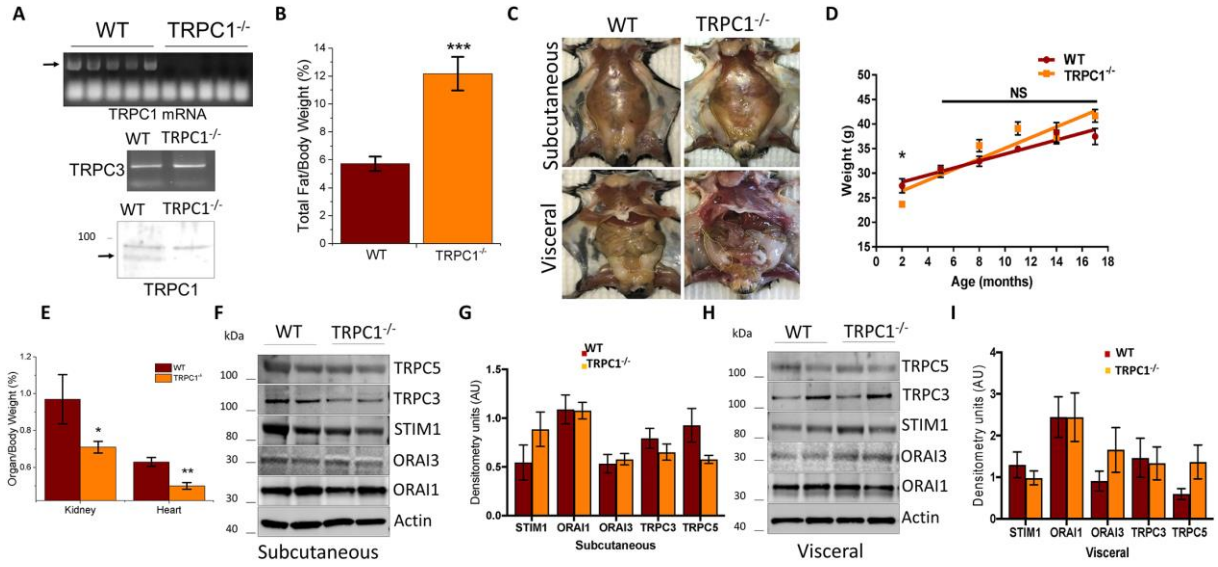

Figure 3: TRPC1$^{-/-}$ mice have increased adiposity with age.

(A) mRNA expression of TRPC1 and TRPC3 from Subc AT of WT and TRPC1$^{-/-}$ mice along with western blot of TRPC1 protein expression. (B) Body fat mass calculated by dividing the fat weight by total body weight of mice aged 13-15 months (n= 9-11). (C) Exposed Subc AT and Visc AT of WT and TRPC1$^{-/-}$ male mice aged 9 months. (D) Total body weight of WT and TRPC1$^{-/-}$ mice by 3-month age groups (n=8-15 for each age). (E) Ratio of organ to total body weight of WT and TRPC1$^{-/-}$ mice. (n=6-10). Western blot of TRPC5, TRPC3, STIM1, ORAI3, and ORAI1 protein expression of Subc AT (F,G) and VAT (H,I) tissue lysates (n=6-8). Graphs are mean ± SEM, significance: *, $p < 0.05$; **, $p < 0.01$; ***, $p < 0.001$ either using T-test or ANOVA.

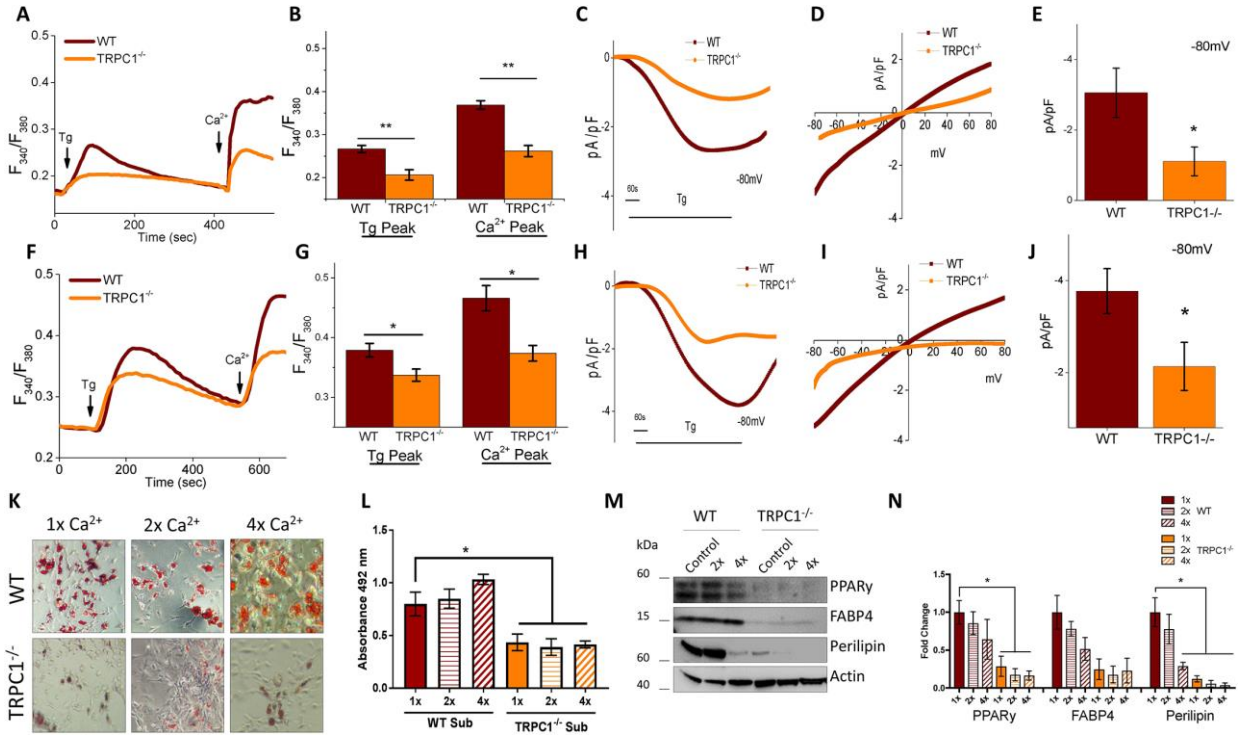

Figure 4: Loss of TRPC1 in Subc adipocytes reduces SOCE and adipogenesis.

Fura-2 traces of transient increase in $[Ca^{2+}]_i$ after addition of 1 µM Tg and 1 mM Ca^{2+} to WT and TRPC1$^{-/-}$ Subc AT SVF (A) and differentiated Subc AT (F). Bar diagram quantifies Tg and Ca^{2+} peaks for Subc AT SVF cells (B) and differentiated Subc AT (G). Each bar gives the mean ± SEM of 40–60 cells in three separate experiments. Application of 1 µM Tg induced inward currents at −80mV in WT and TRPC1$^{-/-}$ Subc AT SVF (C) and differentiated Subc AT (H). Respective IV curves of Subc AT SVF (D) and differentiated Subc AT (I). Quantification (n = 5 recordings) of current intensity at −80 mV is shown for Subc AT SVF in (E) and differentiated Subc AT in (J). (K) Oil-red-o staining (using 10X objective) of WT and TRPC1$^{-/-}$ Subc AT differentiated in 1x (basal), 2x, or 4x extracellular Ca^{2+} for 7 days. (L) Quantification of eluted oil-red-o stain at 492nm (n=7). (M) Western blot of PPARγ, FAPB4, and Perilipin protein expression of WT and TRPC1$^{-/-}$ Subc AT differentiated in 1x (basal), 2x, or 4x extracellular Ca^{2+} with quantification in (M) (n=3) Graphs are mean ± SEM, significance: *, $p < 0.05$; **, $p < 0.01$ using ANOVA.

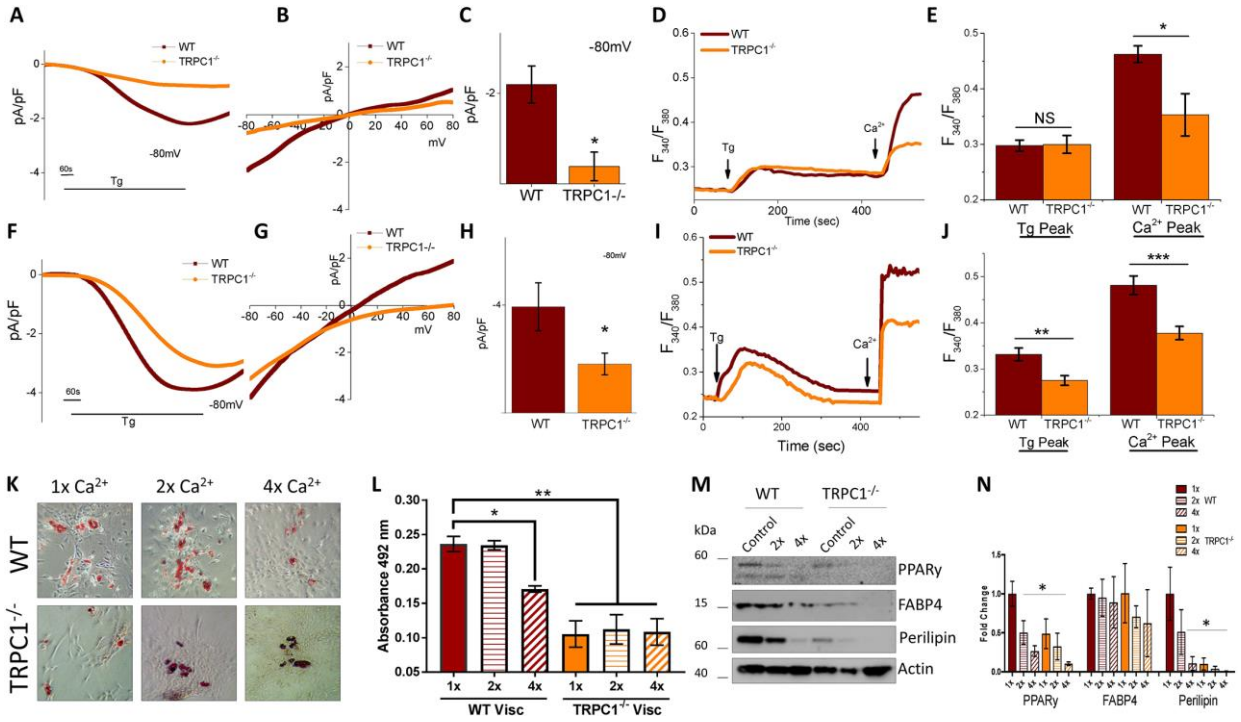

Figure 5: Visceral adipocytes from TRPC1$^{-/-}$ have reduced SOCE and ability to differentiate.

Application of 1 µM Tg induced inward currents at −80mV in WT and TRPC1$^{-/-}$ treated VAT SVF (A) and differentiated Subc AT (F). Respective IV curves shown for VAT SVF (B) and differentiated VAT (G). Quantitation (n = 8 recordings) of current intensity at −80 mV for VAT SVF (C) and differentiated VAT (H). Fura-2 traces of transient increase in $[Ca^{2+}]_i$ after addition of 1 µM Tg and 1 mM Ca^{2+} to WT and TRPC1$^{-/-}$ VAT SVF (D) and differentiated VAT (I). Bar diagram quantifies Tg and Ca^{2+} peaks for VAT SVF (E) and differentiated VAT (J). Each bar gives the mean ± SEM of 40–60 cells in three separate experiments. (K) Oil-red-o staining (using 10x objective) of WT and TRPC1$^{-/-}$ VAT differentiated in 1x(basal), 2x, or 4x extracellular Ca^{2+} for 7 days. (L) Quantification of eluted oil-red-o stain at 492nm (n=4). (N) Western blot of PPARγ, FAPB4, and Perilipin protein expression of WT and TRPC1$^{-/-}$ VAT differentiated in 1x(basal), 2x, or 4x extracellular Ca^{2+} with quantification in (M) (n=). Graphs are mean ± SEM, significance: *, $p < 0.05$; **, $p < 0.01$; ***, $p < 0.001$ using ANOVA.

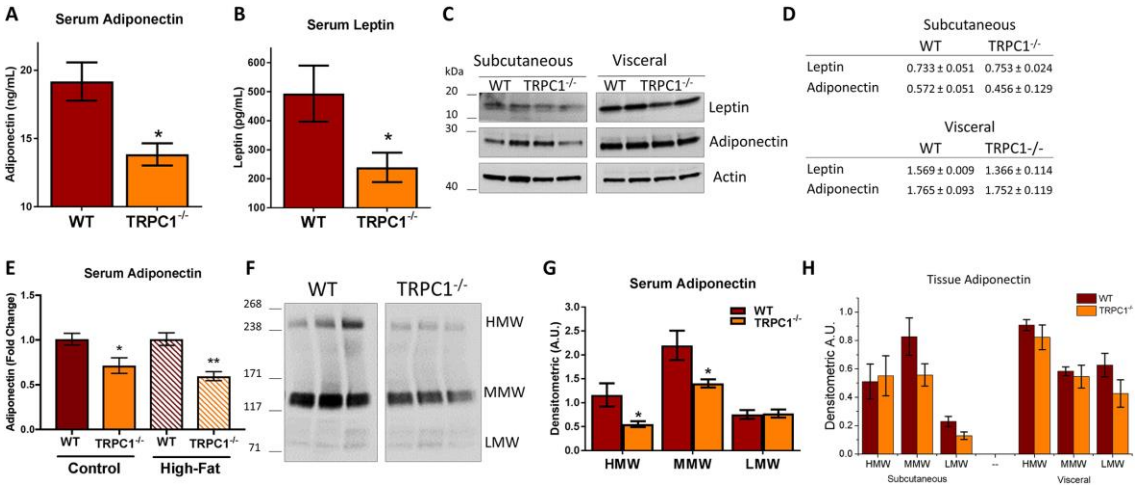

Figure 6: Serum adipokines and isoforms are altered in TRPC1$^{-/-}$ mice.

Elisa assessed total serum adiponectin (A) and leptin (B) of WT and TRPC1$^{-/-}$ mice aged 3-9 months, adiponectin (n=6), leptin (n=8). (C) Western blot of leptin and adiponectin protein expression normalized to actin of WT and TRPC1$^{-/-}$ tissue lysates of Subc AT and VAT and quantified (D) (n=3). (E) Total serum adiponectin from WT and TRPC1$^{-/-}$ mice fasted overnight after 12 weeks on normal chow (16% fat) or high fat (45% fat), (n=8). Serum adiponectin isoforms (F) assessed by non-denaturing PAGE. Optical density of each isoform (HMW (high molecular weight), MMW (middle molecular weight), LMW (low molecular weight)) normalized to total protein from respective Ponceau S stains and quantified (G) (n=4). (H) Non-denaturing PAGE of Subc AT and VAT protein tissue lysates and quantified (n=4). Graphs are mean ± SEM, significance: *, $p < 0.05$; **, $p < 0.01$ either using T-test or ANOVA.

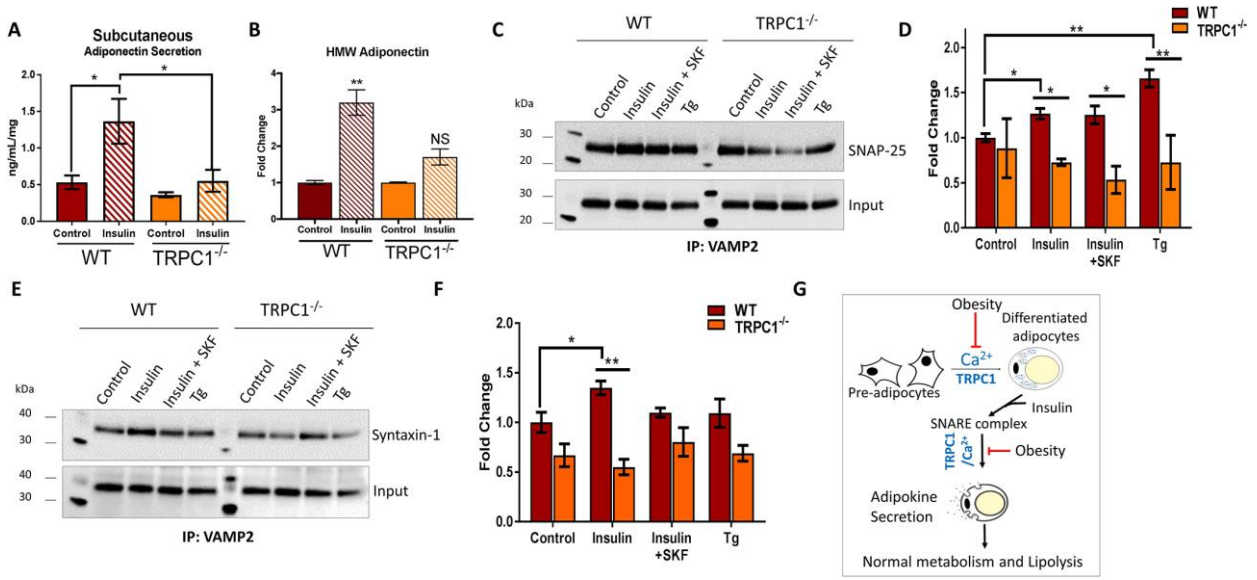

Figure 7: Reduced SNARE protein interactions in TRPC1$^{-/-}$ adipose tissue.

(A) Adiponectin secreted from Subc AT samples from WT and TRPC1$^{-/-}$ stimulated with insulin (100 nM) for 6 hours, n=8. (B) Quantification of HMW adiponectin isoform secreted from (A) (n=4). Co-immunoprecipitation assay of SNARE complexes in Subc AT and VAT lysates from WT and TRPC1$^{-/-}$ stimulated with insulin (100 nM), SKF (10 µM), or Tg (1 µM). Western blot analysis was performed using anti-Vamp2 antibody after immunoprecipitating with anti-SNAP25 (C, quantification in D) and anti-Syntaxin-1 (E, quantification in F) antibodies (n=3). Graphs are mean ± SEM, significance: *, $p < 0.05$; **, $p < 0.01$ using ANOVA. (G) Shows the proposed model where TRPC1 regulate obesity by initiating adipose differentiation and adipokine secretion required for normal metabolism.